The 8th Pacific Rim International Congress on Advanced Materials and Processing
Edited by: Fernand Marquis
TMS (The Minerals, Metals & Materials Society), 2013

INTERFACIAL PROPERTIES OF Ti-6Al-4V/SCS-6 CONTINUOUS FIBRE REINFORCED COMPOSITE

Matthew Dear[1], Timothy Doel[1], Paul Bowen[1], Phillip Doorbar[2]

[1]School of Metallurgy and Materials, University of Birmingham, Edgbaston, Birmingham, B15 2TT, UK

[2]Rolls-Royce plc, PO Box 31, Derby, Derbyshire, DE24 8BJ, UK

Keywords: MMC, Interface, Fatigue, Titanium, Push Out.

Abstract

A study of the interfacial properties of a SiC (SCS-6) fibre reinforced Ti-6Al-4V metal matrix composite has been carried out using a fibre push out technique. Material in the as received condition, heat treated at 300˚C, and some fatigue damaged conditions were considered. Fatigue was performed in 3-point bending at two initial ΔK_{app} levels at both room temperature and 300˚C. To investigate the effect of fatigue on the interfaces, samples were taken from immediately next to the fatigue crack plane, as well as from three positions at increasing distances from the crack plane.

Interfacial properties were significantly reduced by fatigue. Interfacial properties after fatigue were lowest close to the crack plane, and increased at distances further from the crack plane. In the as received condition interfacial debonding occurred between the fibre coating layers. However fatigue and heat treatment caused interfacial damage and promoted debonding between coating layers and within the reaction zone.

Introduction

Continuously reinforced titanium metal matrix composites (TMCs) have gained significant research interest since their conception. The aerospace industry has driven the majority of this research, specifically for use in gas turbine engines, as TMCs have desirable properties such as high specific strength and stiffness. These components are often limited by fatigue.

Fibres play a key role in improving the fatigue crack growth resistance of TMCs over monolithic alloys [1, 2]. To achieve the high crack growth resistance fibres must remain intact to allow bridging in the crack wake [2]. Load is transferred to the fibres and crack tip driving forces are reduced [3, 4, 5]. Fatigue crack growth rates can then decrease as the crack grows and may even arrest [1, 2, 6]. This requires debonding of the fibre/matrix interface and subsequent sliding to occur. Therefore the interfacial properties are important. The stress required for the interfacial debonding, and the stress then needed for sliding against friction can be investigated using a fibre push out technique [7, 8].

This study aims to characterize the interfacial properties of a single TMC system, and the effect of heat treatment and of fatigue at room and elevated temperatures on these properties. A series of fatigue and fibre push out experiments, have been used.

Experimental

Material

The material used in this study was an eight-ply Ti-6Al-4V/SCS-6 composite. Matrix coated fibres were consolidated with cladding material by hot isostatic pressing, forming a fully dense 1.9 mm thick plate with a fibre volume fraction of 35%.

Three-Point Bend Fatigue

Fatigue samples were cut from the composite such that the specimen length was parallel to the fibre direction. Sample dimensions were 4 × 75 × 1.9 mm with a through thickness single edge notch cut at the centre point to a depth of 0.4 mm giving an a_o/W of 0.1.

Three-point bend fatigue was carried out on an Instron servo hydraulic machine fitted with a 5 kN load cell. A sinusoidal waveform was used to load the sample at a frequency of 4 Hz and a stress ratio (R) of 0.1. Initial applied ΔK (ΔK_{app}) of 18, 21, and 23 MPa$\sqrt{m}$ were used at room temperature and 300˚C to promote conditions for both fibre bridging and failure.

Push Out Testing

A continuous loading fibre push out technique was used to identify interfacial properties. Samples were prepared for fibre push out testing by cutting slices of thickness ≈0.5 mm, using a 0.15 mm thick diamond blade, perpendicular to the fibre direction. Slices were polished down to a 3 µm finish and a final slice thickness of 0.2 – 0.35 mm. One sample was prepared in the as received state and three samples after heat treatment at 300˚C for 140 hours. The time of 140 hours was used as this was the time of the longest running fatigue test. Slices were also prepared from each fatigue test piece after testing. The first slice was taken as close to the fatigue crack plane as possible then the subsequent three slices were taken 0.65 mm from one another giving the desired 0.5 mm slice thickness.

Testing was carried out on an ESH servo hydraulic machine fitted with a 1kN load cell, working on a 100 N range. The required fibre was located under a 100 µm diameter indenter using a Questar QM100 optical telescope. The fibre was pushed into a groove in a support block, as shown in Figure 1, at a constant displacement rate of 50 µm/min. 15 fibres were sequentially pushed in a single row along the length of each slice.

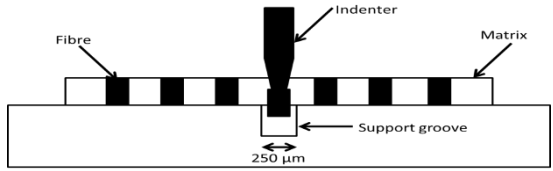

Figure 1. Schematic showing the fibre push out technique.

Interfacial debonding and friction stresses were calculated from the load/displacement trace recorded for each pushed out fibre. Debonding stress was calculated using Equation 1, and the frictional stress was calculated using Equation 2. The interfacial debond stress was taken from the load at the point the fibre started to slide, and the interfacial friction stress was taken from the highest load achieved after debonding.

$$\tau_d = \frac{P_d}{\pi d t} \qquad \text{(Equation 1)}$$

$$\tau_{f=}\frac{P_m}{\pi d(t-u)} \quad \text{(Equation 2)}$$

P_d refers to the debond load, P_m refers to the instantaneous load at the displacement (t – u), d is the fibre diameter, t is the sample thickness.

Results and Discussion

Interfacial Characterization

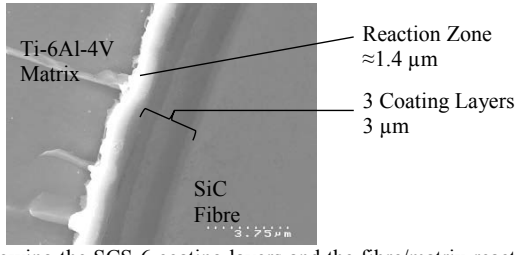

Figure 2. SEM micrograph showing the SCS-6 coating layers and the fibre/matrix reaction zone in the as received condition.

The interfacial microstructure shown in Figure 2 shows 3 individual layers within the fibre coating and a reaction zone. The coating layers are formed of a carbon matrix with varying levels of SiC particles. Layers 1 and 3 are thicker and each has distinct regions of different compositions within them, so in reality there are 6 layers [9].

As Received/Heat Treated Interfacial Properties

Interfacial properties for the as received and heat treated conditions are outlined in Table 1. Both as received and heat treated samples display a friction stress (157 and 168 MPa respectively) higher than the debond stress (102 and 128 MPa respectively). Also, heat treatment in air at 300˚C/140 hours resulted in an increase in interfacial debond stress and a smaller increase in interfacial friction stress.

Table 1. Average interfacial debond and interfacial friction stresses for as received and heat treated samples.

Sample	**Sample Thickness (µm)**	**Debond Stress (MPa)**	**Friction Stress (MPa)**
As Received	220	102	157
Heat Treated (300˚C/140h)	215-268	128	168

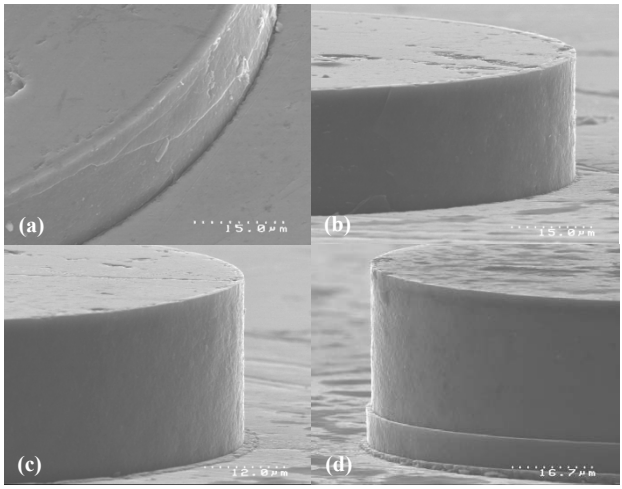

Figure 3. SEM images showing the surfaces of pushed out fibres in the as received condition (a) and after 140 hours at 300˚C (b-d).

Figure 3 shows examples of pushed out fibres in the as received and heat treated conditions. In the as received condition all the fibres tested debonded between the outer coating layer and the reaction zone, as shown in Figure 3 (a). There are no coating layers attached to the matrix, only the reaction zone remains. Conversely the heat treated samples displayed a number of interfacial debond locations, Figure 3 (b-d).

60% of heat treated fibres debonded in the same position, Figure 3 (b), as the as received samples and possessed similar average debond (112 MPa) and friction (165 MPa) stresses. The remaining fibres debonded either between the inner coating layers, Figure 3 (c), or had multiple debond locations, Figure 3 (d). These fibres tended to have slightly higher debond and friction stress.

Interfacial Properties Following Fatigue Loading

Figure 4 shows how interfacial properties change with distance from the fatigue crack plane. Three point bend fatigue reduced both the interfacial debond (a) and friction (b) stress. This reduction was greatest close to the fatigue crack plane. Both debond stress, Figure 4 (a), and friction stress, Figure 4 (b), increased towards as received values as the distance from the crack plane increased. This finding is in line with those of Sinclair *et al* [4] where a linear decrease in friction stress was found as distance to the crack plane reduced. Figure 4 (a) shows the effect of temperature on debond stress is greater at low initial ΔK_{app}; and there is a larger reduction in interfacial debond stress cause by temperature at initial ΔK_{app} of 18 MPa$\sqrt{m}$ than at the higher values. Likewise the effect of increasing the initial ΔK_{app} is larger at room temperature than at 300˚C. In samples taken closest to the crack plane higher initial ΔK_{app} levels reduce the interfacial debond stress to a greater extent than at larger distances.

Figure 4 (b) shows that increasing the fatigue test temperature causes a similar reduction of interfacial friction stress at both high and low initial ΔK_{app} levels. The effect of initial ΔK_{app} levels on friction stress is small at both room temperature and 300˚C; with the exception of the room temperature results closest to the crack and 300˚C results ≈1.8 mm from the crack.

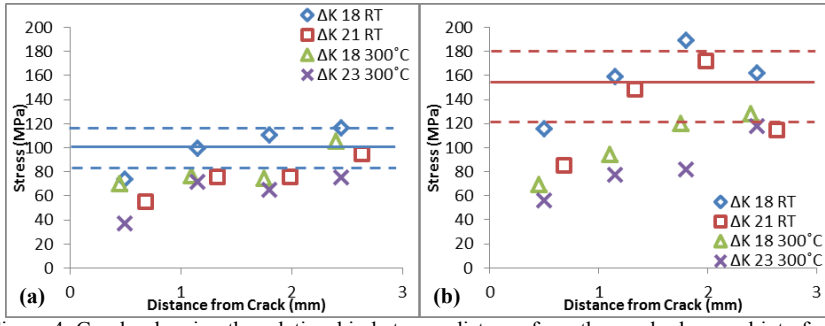

Figure 4. Graphs showing the relationship between distance from the crack plane and interfacial debond stress (a) and interfacial friction stress (b), for samples that experienced fatigue at high and low initial ΔK_{app} at room temperature (RT) and 300˚C. The horizontal coloured lines represent the range and average for the as received condition.

Interfacial debond and friction stresses shown in Figure 4 are averaged for each slice. Figure 5 shows the sequential fibre to fibre distribution of interfacial properties for slices taken closest to the fatigue crack plane for each condition. With the exception of four fibres in Figure 5 (c), initial ΔK_{app} = 18 MPa√m at 300˚C, fatigue under all conditions resulted in both interfacial debond and friction stresses being reduced below the average as received values.

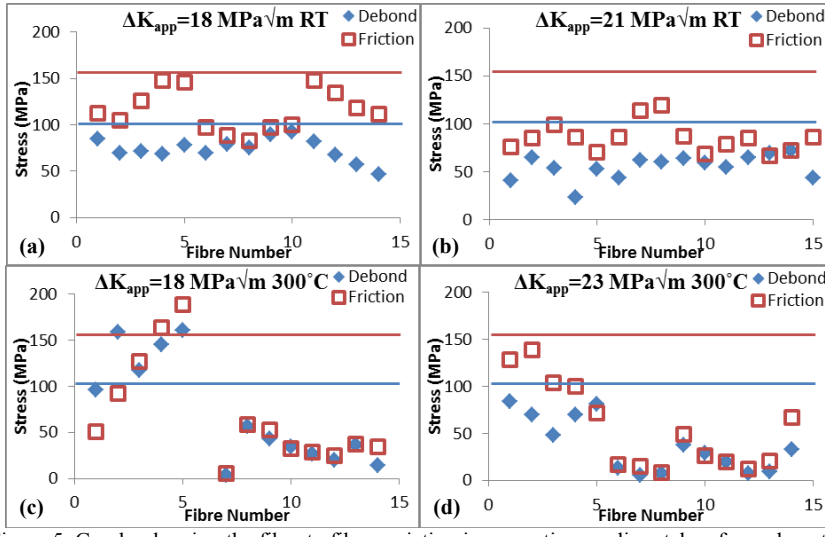

Figure 5. Graphs showing the fibre to fibre variation in properties on slices taken from closest to the fatigue crack plane (a=0.5, b=0.68, c=0.45, d=0.5 mm) that have experienced fatigue at low (a, c) and high (b, d) initial ΔK_{app} at room temperature (RT) (a, b) and 300˚C (c, d). The horizontal coloured lines represent the as received averages.

Samples fatigued at room temperature, Figure 5 (a, b), displayed no spatial correlation with interfacial properties. However samples fatigued at 300˚C, Figure 5 (c, d), both display two regions; one with very low interfacial properties with similar friction and debond stresses, the second region with higher properties and the friction stress is usually higher than the debond stress.

Figure 6 shows pushed out fibres from fatigued samples. After fatigue at room temperature, fibres debonded either between the carbon coating layers or between the outer carbon coating layer and the reaction zone, Figure 6 (a). There was no apparent correlation between the debonding position and the position of the fibre within the slice.

After fatigue at 300˚C, in the region with low interfacial properties in Figure 5 (c, d), the fibre appearance after push out was often that shown in Figure 6 (b). The severity of the vertical groove like features was greatest in slices from close to the crack plane. At room temperature such damage was only limited, Figure 6 (c). For fibres with higher interfacial properties in Figure 5 (c, d), several different debond positions were observed. In addition to those found in fibres fatigued at room temperature, interfacial debonding within the reaction zone was found, see Figure 6 (d).

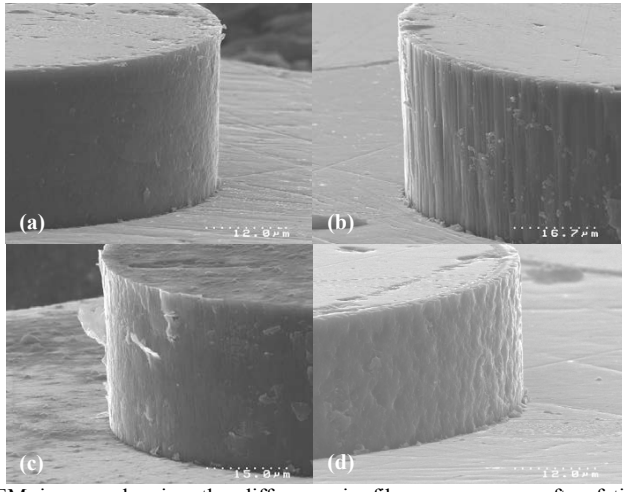

Figure 6. SEM images showing the difference in fibre appearance, after fatigue at room temperature (a, c) and at 300˚C (b, d).

The two distinct regions observed in Figure 5 (c, d) for samples fatigued at 300˚C are the regions through which the fatigue crack grew (the fatigue region) and the region where the testpiece finally failed at the end of the fatigue test (fracture region). Fibres in the fatigue region show low interfacial properties and similar debond and friction stresses. This debond stress is actually an overcoming of sticking friction as these fibres debonded during the fatigue process. Interfacial debonding and fibre bridging during fatigue results in repeated interfacial sliding between fibre and matrix. This process would have caused the damage observed in Figure 6 (b). It should be noted that this damage was more severe in the sample taken from close to the crack plane.

However no such trend was observed after fatigue at room temperature, Figure 5 (a, b). At 300˚C thermal residual stresses are lower and therefore the effect of matrix clamping on the fibre is reduced. Also the modulus of the matrix will be reduced. Therefore crack opening displacements will be larger during fatigue at 300˚C and more interfacial sliding will occur. Hence debonding will extend further along the fibres away from the crack plane during fatigue at 300˚C than at room temperature. It is likely that the slices shown in Figure 5 (c) and (d), 0.45 and 0.5 mm from the respective crack planes were taken from inside the debonded length. The slices taken from test pieces fatigued at room temperature, shown in Figure 5 (a) and (b), 0.5 and 0.68 mm from the respective crack planes, were taken from outside the shorter debonded region, even at high ΔK_{app}, and hence no distinction between the fatigue and fracture regions can be made.

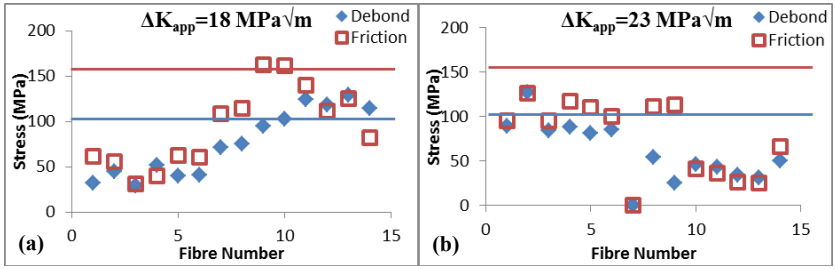

Figure 7. Graphs showing the fibre to fibre variation for fatigue effected samples at 300˚C at a low (a) and high (b) initial ΔK_{app}. Samples were the furthest from the crack plane that a clear fatigue and fracture region could be identified from the properties alone. (a)=1.1 mm, (b)=1.8 mm. The horizontal coloured lines represent the average as received values.

Figure 7 shows that in samples fatigued at 300˚C fatigue and fracture regions could still be identified from interfacial properties in slices taken from larger distances away from the crack plane. For an initial ΔK_{app} of 18 MPa√m this behaviour was exhibited up to 1.1 mm from the crack plane, while increasing the initial ΔK_{app} to 23 MPa√m resulted in this distance from the crack plane increasing to 1.8 mm. At these distances the interfacial damage shown in Figure 6 (b) was not as severe and was only observed in fibres nearer the notch.

Conclusions

1. Heat treatment at 300˚C/140h in air caused a small increase in interfacial properties.
2. Fatigue reduced interfacial properties below as received values. Both interfacial debond and friction stresses were lowest closest to the crack plane.
3. The effect of fatigue at 300˚C compared to room temperature on interfacial debond stress was greatest at lower initial ΔK_{app}, while the effect on friction stress was similar at both initial ΔK_{app}.
4. Interfacial damage accumulated from fatigue was observed in samples fatigued at 300˚C, and reduced with increased distance from the crack plane.
5. Interfacial debonding during fatigue extended further in samples fatigued at 300˚C and in samples with higher initial ΔK_{app}.

Acknowledgements

The authors acknowledge, with thanks, the financial support provided by the Engineering and Physical Science Research Council (EPSRC) and Rolls-Royce plc for provision of material and further financial support.

References

[1] C.Barney, D.C.Cardona and P.Bowen, "Fatigue crack growth resistance from unbridged defects in continuous fibre reinforced metal matrix composites," *International Journal of Fatigue,* vol. 20, no. 4, pp. 279-289, 1998.

[2] R.L.Brett, P.J.Cotterill and P.Bowen, "The influence of loading levels, temperature and environment on fibre failure during the fatigue of an SiC fibre reinforced Ti-MMC," *International Journal of Fatigue,* vol. 18, no. 1, pp. 1-8, 1996.

[3] M.Preuss, G.Rauchs, T.J.A.Doel, A.Steuwer, P.Bowen and P.J.Withers, "Measurementsof fibre bridging during fatigue crack growth in Ti/SiC fibre metal matrix composites," *Acta Materialia,* vol. 51, pp. 1045-1057, 2003.

[4] R.Sinclair, M.Preuss, E.Maire, J.Y.Buffiere, P.Bowen and P.J.Withers, "The effect of fibre fractures in the bridging zone of fatigue cracked Ti-6Al-4V/SiC fibre composite," *Acta Materialia,* vol. 52, pp. 1423-1438, 2004.

[5] Y.C.Hung, J.A.Bennett, F.A.Garcia-Pastor, M. Michiel, J.Y.Buffiere, T.J.A.Doel, P.Bowen and P.J.Withers, "Fatigue crack growth and load redistribution in Ti/SiC composites observed in situ," *Acta Materialia,* vol. 57, pp. 590-599, 2009.

[6] A.R.Ibbotson, C.J.Beevers and P.Bowen, "Damage assessment and lifing of continuous fibre-reinforced metal-matrix composites," *Composites,* vol. 3, pp. 241-247, 1993.

[7] J.M.Yang, S.M.Jeng and C.J.Yang, "Fracture mechanisms of fibre-reinforced titanium alloy matrix composites Part I: Interfacial behaviour," *Materials Science and Engineering,* vol. 138, pp. 155-167, 1991.

[8] K.Fox, "Effects if interfacial properties of fatigue crack growth resistance in Ti/SiC metal matrix composites," PhD Thesis University of Birmingham, 1995.

[9] X.J.Ning and P.Pirouz, "The microstructure of SCS-6 SiC fibre," *Journal of Materials Research,* vol. 6, no. 10, pp. 2234-2248, 1991.